

Study the Structural and Optical behaviour of Conducting Polymer based nanocomposites: ZrO₂-Polypyrrole Nanocomposites

Gaganpreet Kaur Sidhu and Rajesh Kumar*

Department of Physics, Panjab University, Chandigarh- 160014, India

*Corresponding author Email: rajeshbaboria@gmail.com

Abstract. Conducting polymer provides an intriguing type of environment for various inorganic structures resulting in the generation of exciting properties in the composite owing to the mutual interactions between the two and this provides interesting dimensions for the development of new multifunctional devices. ZrO₂ ceramic is one of the most investigated materials for its outstanding mechanical properties ionic, conduction properties and due to its high oxygen ion conduction. In order to achieve novel properties of ZrO₂ nanoparticles, nanocomposites of ZrO₂ with Polypyrrole (PPy) were prepared through in-situ method using ZrO₂/pyrrole dispersions. Firstly, ZrO₂ nanoparticles were synthesized by co-precipitation method and then embedded in pyrrole solution for polymerization. The structural and optical properties of ZrO₂/PPy nanocomposites were investigated comprehensively by X-Ray diffraction (XRD), UV-visible spectroscopy and Fourier-transform infrared spectroscopy (FTIR). XRD and FTIR highlight the presence of tetragonal phase of ZrO₂ nanoparticles in nanocomposites, whereas UV-Visible and PL spectra indicate the presence of different electronic levels.

1. Introduction

During the recent years there has been an explosive growth in the field of nanocomposites. It represents a new class of materials having improved properties as compared to pure conducting polymers and metal oxides¹. These nanocomposites possess interesting electrical and potential applications in the fields like chemical sensors, biosensors, electronic devices, etc²⁻⁴. Such materials are of great interest both in the field of physics and chemistry due to their novel properties, which are entirely different from that of constituents^{5,6}. There are number of examples regarding polymer/metal oxide hybrid materials in which polymers such as polystyrene⁷ and poly (vinyl chloride)⁸ are combined with metal oxides or salts such as CuO, SiO₂⁹, ZrO₂¹⁰, BaSO₄¹¹. Polymeric materials can be obtained in different form depending on the requirement for various applications like in powder form, thin films, nanorods, etc. Several methods have been used by researchers to improve the properties of polymers, among them one of the best methods is the synthesis of polymer/metal oxide nanoparticles. Polymer/metal oxides acquired an important part in the present technology. Among various conducting polymers, Polypyrrole (PPy) has attracted much attention due to its unique electrical properties like electrical conductivity and is environmental friendly nature¹². PPy can be easily prepared either by oxidative chemical or electrochemical polymerization of pyrrole. PPy has been used in biosensors,^{13,14} gas sensors,^{15,16} wires,¹⁷ microactuators,¹⁸ and anti-electrostatic coatings¹⁹. Metal oxides materials provide good mechanical strength and stability to the polymers. However, among different metal oxides, we use ZrO₂. It is an



excellent oxide material with wide band gap (5 - 7 eV). It exists in three different forms Monoclinic (Room temperature-1170 °C), Tetragonal (1170-2370°C) and Cubic (above 2370°C. The most important phase of ZrO₂ for application point of view is tetragonal phase which can be stabilized at low temperature by number of methods²⁰. It possesses various applications such as fuel sensors, oxygen sensors²⁰, catalyst²¹ etc. All these properties are mainly due to high specific surface area and presence of oxygen vacancies²². Here, we report the synthesis of polymer/metal oxide nanocomposites comprising PPy as the polymer and ZrO₂ as the metal oxide component. PPy/ZrO₂ nanocomposites were synthesized by embedding synthesized ZrO₂ nanoparticles into a PPy matrix during the polymerization of pyrrole and studied their structural and optical properties.

2. Experimental Details

Pyrrole, ferric chloride hexahydrate and distilled water all were obtained as AR grade reagents commercially are used for the synthesis of PPy. PPy was synthesized by chemical oxidative polymerization using pyrrole as the monomer and ferric chloride hexahydrate as the oxidizing agent. Polymerization was carried out in a beaker by mixing 1 ml of vacuum distilled pyrrole with 100 ml of distilled water containing 9.74 gm of ferric chloride hexahydrate at room temperature. The optimal ratio of Fe (III)/ monomer is 2.5. The solution was stirred for 24 hrs on magnetic stirrer giving rise to the formation of black precipitates. These precipitates were then filtered with the help of vacuum and washed with the copious amount of deionised water until the solution becomes clear. Precipitates were dried overnight in air and then again dried in oven at 25°C.

PPy/ZrO₂ nanocomposites has been synthesized by adding 1 ml of vacuum distilled pyrrole to 100 ml of distilled water containing 9.74 g of ferric chloride hexahydrate and ZrO₂ nanoparticles at room temperature. The solution was stirred for 24 hrs on magnetic stirrer which gave rise to the formation of black precipitates followed by the same procedure as mentioned above.

X-Ray diffraction (XRD) patterns were recorded on a Philips PW-3710 diffractometer using Cu K α radiation ($\lambda = 1.5406 \text{ \AA}$) in the 2θ range $10^\circ - 80^\circ$ to determine the crystal structure and estimate the average crystallite size. Fourier-transform IR (FTIR) spectra ($4000 - 400 \text{ cm}^{-1}$) were recorded for the prepared powder to confirm the formation of composite. UV-Visible and PL spectra of PPy, and PPy/ZrO₂ nanocomposites were recorded to understand the absorption and emission spectra of polymer and nanocomposites.

3. Results and Discussion

Figure 1 shows the XRD patterns of pure PPy and ZrO₂/PPy nanocomposites. A broad peak at around $2\theta = 25.12^\circ$ indicating the short range ordering of PPy powders, which assigned to the repeated units of pyrrole ring, implying that polymer chain is highly oriented²³. However, the XRD pattern of ZrO₂/PPy nanocomposites consist some additional peaks that correspond to the tetragonal phase of ZrO₂ nanoparticles. Peaks at $2\theta = 30.69^\circ$, 50.74° , and 60.27° can be indexed as (1 1 1), (2 0 0) and (2 1 1) crystal planes of ZrO₂ nanoparticles, respectively. The peak positions of nanoparticles are almost at same position as is observed in pure nanoparticles which imply that even in composite, nanoparticles retain their identical structure. However, nanoparticles peaks are not so sharp indicating the amorphous nature of nanocomposites. The average crystallite size has been calculated using basic Scherrer's

$$D = \frac{k\lambda}{\beta \cos \theta}$$

formula given as: $D = \frac{k\lambda}{\beta \cos \theta}$, in which β is the full width at half maximum (FWHM), λ is the X-ray wavelength, θ is the diffraction angle and k is the Scherrer's constant of the order of unity. The average crystallite size of nanoparticles present in nanocomposites has been calculated using basic Scherrer's formula as mentioned above. The average crystallite size has been calculated by fitted all the curves using Gaussian fit. When PPy is polymerized using FeCl_3 , then average crystallite size of globules was found to be 5.8 Å. However, the average crystallite size of nanoparticles in nanocomposites comes out to be ~ 8 nm. The full width half maxima and the average crystallite size corresponding to all peaks are listed in Table 1.

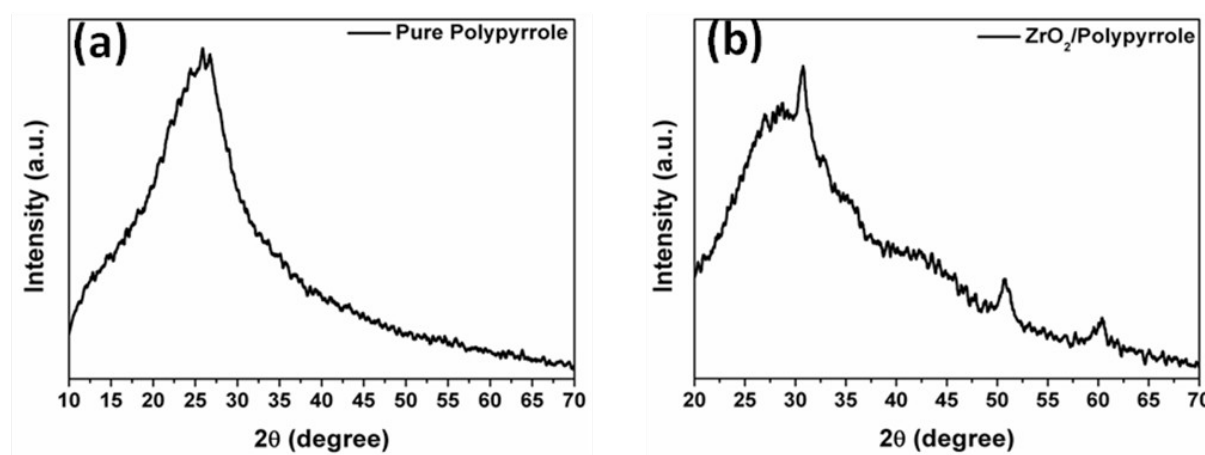


Figure 1: XRD spectra of (a) pure Polypyrrole (PPy) and (b) of ZrO_2 /PPy nanocomposites.

Table 1: Average crystallite size calculated for Pure PPy and ZrO_2 nanoparticles in nanocomposites.

Material	2θ	FWHM (β)	Crystallite Size d (size) (nm)
Polypyrrole	28.56°	14.18	0.58
	30.76°	0.902	8.45
ZrO_2	50.74°	1.171	7.37
	60.29°	2.096	4.45

Figure 2 shows the Fourier transform infrared spectra of pure PPy powder which was recorded using KBR pellets in wavelength range of 4000 to 400 cm^{-1} . The band at 1681 cm^{-1} , 1533 cm^{-1} and weak band at 1447 cm^{-1} are assigned to C–N in plane bending vibration, stretching vibration of C = C and C – C stretching vibration respectively, which may be due to the over oxidization of PPy. PPy shows characteristic peaks of C–H in-plane bending vibration and C–O–C stretching vibration of pyrrole at 1159 cm^{-1} and 1016 cm^{-1} , respectively in the IR spectrum. The band at 1283 cm^{-1} corresponds to the C=N bond and the adsorption band at 858 cm^{-1} corresponds to the out-of plane vibration of the C-H bond²⁴. All peaks correspond to PPy are present in ZrO_2 /PPy nanocomposites FTIR spectra, but with little shifts in peak positions. Peak at 1681 cm^{-1} in PPy shifts to 1672 cm^{-1} , 1533 cm^{-1} shifts to 1525 cm^{-1} ,

1447 cm^{-1} to 1439 cm^{-1} , 1283 cm^{-1} to 1279 cm^{-1} , 1159 cm^{-1} to 1146 cm^{-1} , 1016 cm^{-1} to 1018 cm^{-1} and 858 cm^{-1} to 852 cm^{-1} . All peaks corresponding to their respective bands are listed in Table 2. These shifts in peak positions indicate the presence of interaction between the chains of PPy and nanoparticles. In addition to these peaks, another peak at 752 cm^{-1} is also observed which corresponds to Zr-O bond. ZrO_2 nanoparticles show its characteristics FTIR peak in the range from 500-800 cm^{-1} .

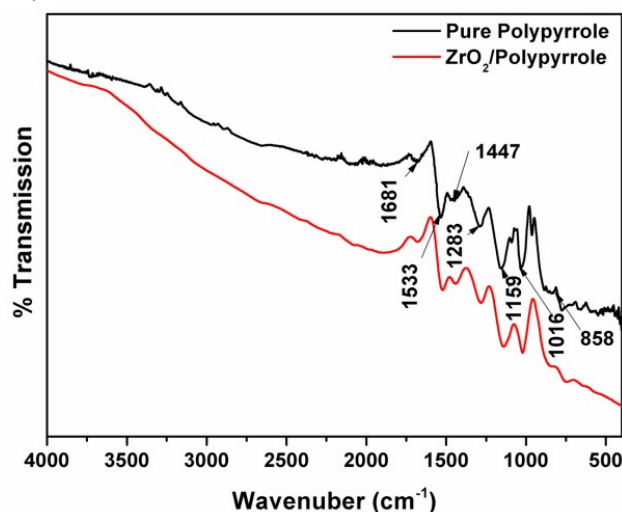


Figure 2: FTIR spectra of pure Polypyrrole (PPy) and ZrO_2 /Polypyrrole nanocomposite.

Table 2: Various FTIR peaks observed in pure PPy and ZrO_2 /Polypyrrole nanocomposite.

Characteristic Bands	Peak positions (cm^{-1})
C-N in plane bending vibration	1681
C = C stretching vibration	1533
C - C stretching vibration	1447
C-H in-plane bending vibration	1159
C-O-C stretching vibration	1016
C=N stretching vibration	1283
C-H bond out-of plane vibration	858
Zr-O vibration	752
O-H vibrations	3500-3000

Figure 3, shows the absorption spectra of pure PPy powder with absorption peak at around 232 nm, whereas ZrO_2 /PPy nanocomposites shows absorption peak at around 234 nm. In literature, UV-Vis peak of PPy was reported at around 340 nm and at 460 nm⁸. In our case only single peak around 232 nm is observed which is due to the transition of electron from the highest occupied molecular orbital (HOMO) to the lowest unoccupied molecular orbital (LUMO) and is related to the $\pi^*-\pi$ electronic transition²⁵. However, in ZrO_2 /PPy nanocomposites a small shift in peak is observed towards the higher wavelength. This relocation in absorption peak reveals a change in electronic structure and transposition of polaron levels in PPy due to the interaction with ZrO_2 nanoparticles. A sizeable overlay of optical transition takes place between PPy and extrinsic states of ZrO_2 nanoparticles^{26,27}.

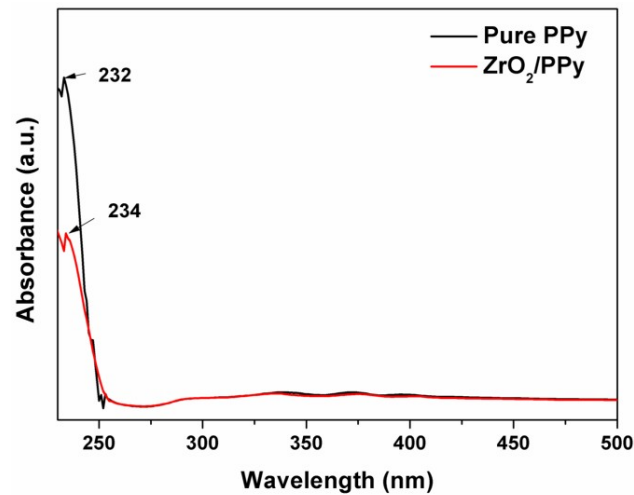


Figure 3: Absorption spectra of Pure PPy and ZrO₂/PPy nanocomposites.

PPy-nanocomposites are amorphous materials and obey Tauc relation. So the band gap of samples has been calculated using UV-Vis spectra as shown in Figure 4. The Tauc relation is

given by: $\alpha h\nu = A(h\nu - E_g)^n$, in which α is known as absorption coefficient, $h\nu$ known as photon energy, E_g is the optical bandgap, and A is constant. The indices n attained different value depending on the type of transitions as $1/2$, $3/2$, 2 , 3 for direct allowed and forbidden or indirect allowed and forbidden transitions, respectively. As shown in Figure 4, the absorbance is plotted against the photon energy for PPy and its composites, a satisfactory fit is obtained for $n = 1/2$, which corresponds to the existence of a direct allowed bandgap. The intercept is drawn to the curve on the photon energy axis gives the bandgap of all the samples. A decrease in bandgap of nanocomposites is observed with the addition of nanoparticles which is due to the alteration of electronic structure. The band gap calculated for pure PPy and ZrO₂/PPy nanocomposites is 6.1 and 5.07 eV, respectively.

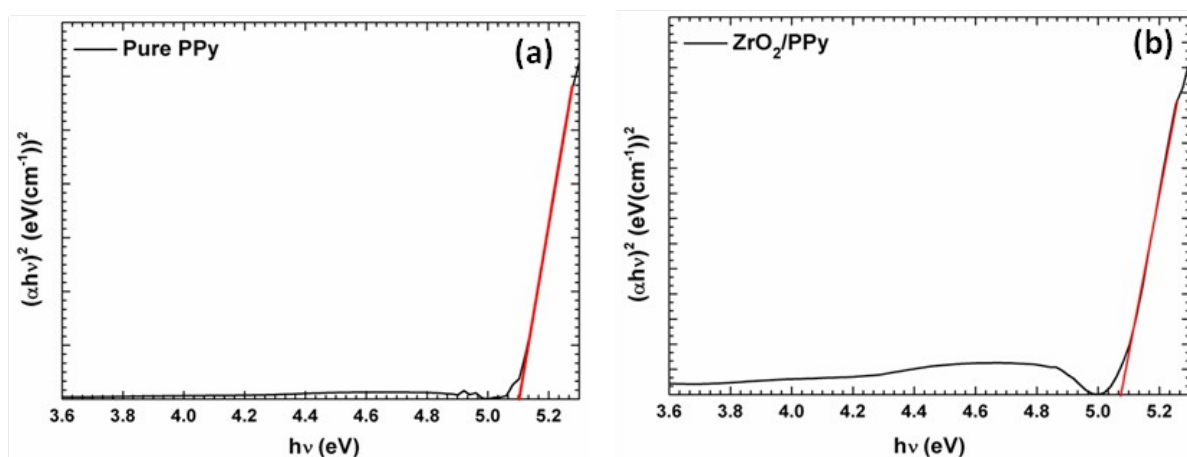


Figure 4: Variation of absorption coefficient with photon energy of (a) Pure PPy and (b) ZrO₂/PPy nanocomposite.

The photoluminescence spectrum of the PPy and its composite were tested and shown in Figure 5. A broad peak centered at 508 nm was collected in pure PPy. ZrO₂/PPy also shows much broader emission peak with lesser intensity as compared to pure PPy which is due to the presence of ZrO₂ nanoparticles²⁸. At 430 nm excitation in the near UV region, both polymer and composite exhibited one strong green emission band at around 508 nm. The presence of PL peak at same position in composite indicates the dominating role of polymer as compared to nanoparticles.

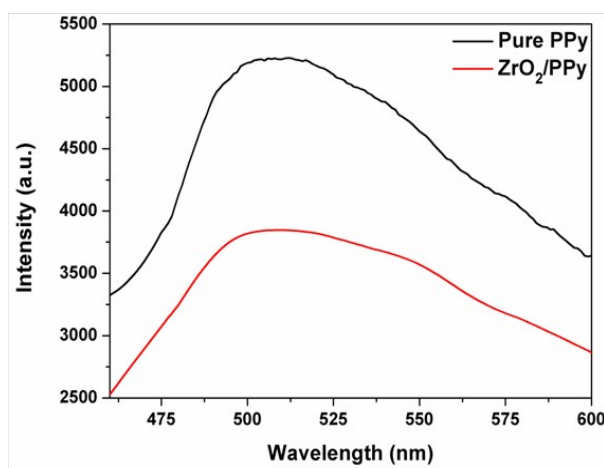


Figure 5: PL spectra of pure PPy and ZrO₂/PPy nanocomposite.

4. Conclusion

ZrO₂/PPy nanocomposites were synthesized by chemically oxidative polymerization. The prepared nanocomposites was analysed for structural and optical properties. XRD reveals the combined broad peak of PPy and various peaks of ZrO₂ nanoparticles in ZrO₂/PPy nanocomposite indicating the presence of tetragonal phase of nanoparticles is still present in nanocomposites. FTIR peaks confirm the formation of composite, whereas optical properties shows absorbance and emission peak of PPy at 232 and 508 nm, respectively with a small shift in both peaks in its composite.

Acknowledgments

The authors are thankful to CIL Department of Panjab University, Chandigarh for various characterizations and IISER, Mohali for PL measurements. One of the authors Ms. Gaganpreet Kaur Sidhu is thankful to UGC for research fellowship.

References

1. Gangopadhyay R and De A 2000 *Chem. Mater.* **12** 608
2. Jiu T, Liua H, Gana H, Li Y, Xiao S, Li H, Liu Y, Lu F, Jiang L and Zhu D 2005 *Synthetic Met.* **148** 313
3. Rein H, Ruckpaul K and Haberditzl W 1973 *Chem. Phys. Lett.* **20** 71
4. Halls J J M, Walsh C A, Greenham N C, Marseglia E A, Friend R H, Moratti S C and Holmes A B 2002 *Nature* **376** 498
5. Sui X, Chu Y, Xing S and Liu C 2004 *Mater. Lett.* **58** 1255

6. Murugendrappa M, Parveen A, and Prasad M A 2007 *Materials Science and Engineering: A* **459** 371
7. Lascelles S F and Armes S P 1995 *Adv. Mater.* **7** 864
8. Banerjee P and Mandal B M *Synthetic Met.* 1995 **74** 257
9. Maeda S and Armes S 1995 *Synthetic Met.* **73** 151
10. Bhattacharya A, Ganguly K M, De A and Sarkar S 1996 *Mater. Res. Bull.* **31** 527
11. Gan L M, Zhang L H, Ghan H S O and Chew C H 1995 *Mater. Chem. Phys.* **40** 94
12. Yao T, Lin Q, Zhang K, Zhao D, Lv H, Zhang J, Yang B 2007 *J. Colloid Interface Sci.* **315** 434
13. Vidal J C, García E and Castillo J R 1999 *Anal. Chim. Acta* **385** 213
14. Gao M, Dai L and Wallace G G 2003 *Electroanal.* **15** 1089
15. Cherenack K and Pieterse L 2012 *J. of Appl. Phys.* **112** 091301
16. Kemp N T, Flanagan G U, Kaiser A B, Trodahl H J, Chapman B, Partridge A C and Buckley R G 1999 *Synthetic Met.* **101** 434
17. Jerome C, Labaye D, Bodart I and Jerome R 1999 *Synthetic Met.* **101** 3
18. Jager E W, Smela E and Ingnas O 2000 *Science* **290** 1540
19. Navale S T, Khuspe G D, Chougule M A and Pati V B 2014 *J. Phys. Chem. Solids.* **75** 236
20. Srinivasan R, De Angelis J, Ice G and Davis B H 1991 *Journal of Materials Research* **6** 1287
21. Su C, Li J, He D, Cheng Z and Zhu Q 2000 *Appl. Catal. A* **202** 81
22. Kumar A M and Rajendran N 2012 *Surf. Coat. Tech.* **213** 155
23. Orinakova R, Fedorkova A and Orinak A 2013 *Chem. Pap.* **67** 860
24. Huyen D N, Tung N T, Vinh T D and Thien N D 2012 *Sensors* **12** 7965
25. Abdulla H S and Abbo A I 2012 *Int. J. Electrochem. Sci.* **7** 10666
26. Dey A and De S 2006 *J. Phys. D. Appl. Phys.* **39** 4077
27. Singh S K and Shukla R 2015 *Mat. Sci. Semicon. Proc.* **31** 245
28. Wang W, Yu D and Tian F 2010 *J. Lumin.* **130** 494